Synthesis and Characterization of Phosphorescent Cyclometalated Iridium Complexes

Sergey Lamansky, Peter Djurovich, Drew Murphy, Feras Abdel-Razzaq, Raymond Kwong, Irina Tsyba, Manfred Bortz, Becky Mui, Robert Bau, and Mark E. Thompson*

Department of Chemistry, University of Southern California, Los Angeles, California 90089

Received August 8, 2000

The preparation, photophysics, and solid state structures of octahedral organometallic Ir complexes with several different cyclometalated ligands are reported. $IrCl_3 \cdot nH_2O$ cleanly cyclometalates a number of different compounds (i.e., 2-phenylpyridine, 2-(*p*-tolyl)pyridine, benzoquinoline, 2-phenylbenzothiazole, 2-(1-naphthyl)benzothiazole, and 2-phenylquinoline), forming the corresponding chloride-bridged dimers, $\underline{C\wedge N}_2Ir(\mu\text{-}Cl)_2Ir\underline{C\wedge N}_2$ ($\underline{C\wedge N}$is a cyclometalated ligand) in good yield. These chloride-bridged dimers react with acetyl acetone (acacH) and other bidentate, monoanionic ligands such as picolinic acid (picH) and *N*-methylsalicylimine (salH), to give monomeric $\underline{C\wedge N}_2Ir(LX)$ complexes (LX = acac, pic, sal). The emission spectra of these complexes are largely governed by the nature of the cyclometalating ligand, leading to λ_{max} values from 510 to 606 nm for the complexes reported here. The strong spin−orbit coupling of iridium mixes the formally forbidden ^{3}MLCT and $^3\pi-\pi^*$ transitions with the allowed ^{1}MLCT, leading to a strong phosphorescence with good quantum efficiencies (0.1−0.4) and room temperature lifetimes in the microsecond regime. The emission spectra of the $\underline{C\wedge N}_2Ir(LX)$ complexes are surprisingly similar to the *fac*-$Ir\underline{C\wedge N}_3$ complex of the same ligand, even though the structures of the two complexes are markedly different. The crystal structures of two of the $\underline{C\wedge N}_2Ir(acac)$ complexes (i.e., $\underline{C\wedge N}$ = *ppy* and *tpy*) have been determined. Both complexes show *cis*-C,C′, *trans*-N,N′ disposition of the two cyclometalated ligands, similar to the structures reported for other complexes with a "$\underline{C\wedge N}_2Ir$" fragment. NMR data (^{1}H and ^{13}C) support a similar structure for all of the $\underline{C\wedge N}_2Ir(LX)$ complexes. Close intermolecular contacts in both $(ppy)_2Ir(acac)$ and $(tpy)_2Ir(acac)$ lead to significantly red shifted emission spectra for crystalline samples of the *ppy* and *tpy* complexes relative to their solution spectra.

Introduction

The photophysics of octahedral $4d^6$ and $5d^6$ complexes has been studied extensively.[1] These complexes, particularly those prepared with Ru^{2+} and Os^{2+}, have been used extensively in photocatalysis and photoelectrochemistry.[2] The reason these d^6 complexes are attractive in photochemical applications is that they have long-lived excited states and good photoluminescence efficiencies. The majority of the studies have been focused on the photophysical properties of octahedral metal−diimine complexes Ru^{2+} and Os^{2+}, with ligands such as the bipyridine and phenanthroline.[3] More recently a number of groups have investigated the isoelectronic Rh^{3+} and Ir^{3+} complexes.[4] Tris-chelate complexes of Rh and Ir have been prepared with diimine ligands as well as cyclometalated ligands, such as 2-phenylpyidinato-C^2,N (*ppy*).[5] Several tris-cyclometalated complexes of Rh and Ir have been reported, e.g., *fac*-M(*ppy*)$_3$, *fac*-M(2-(2-thienyl)pyridine)$_3$.[6] The cyclometalated ligands are monoanionic, thus forming neutral metal tris-chelate complexes, which are isoelectronic to the cationic Ru and Os complexes. When both cyclometalated and diimine ligands are used, monocationic complexes can be obtained, e.g., $(ppy)_2M(L')^+$ (L′ = 2,2′-bipyridine, phenanthroline).[7]

Both neutral and cationic tris-chelate complexes of Rh and Ir show excited state lifetimes in the microsecond regime, as expected for a high-spin excited state. The Ir complexes show intense phosphorescence at room temperature, while the Rh complexes give measurable emission only at low temperatures. The stronger spin−orbit coupling expected for Ir relative to Rh significantly mixes singlet and triplet excited states for Ir, largely removing the spin-forbidden nature of the phosphorescent transitions, leading to efficient phosphorescence for these complexes [e.g., ϕ_{phos}(*fac*-Ir(*ppy*)$_3$) = 0.4].[9] The phosphorescent lifetimes for these Ir complexes are relatively long ($\tau \approx \mu$s),[4−7] compared to fluorescent lifetimes, which are typically in the

* Author to whom correspondence should be addressed. E-mail: met@usc.edu.

(1) (a) Balzani, V.; Scandola, F. *Supramolecular Photochemistry*; Ellis Horwood: Chichester, U.K., 1991. (b) Balzani, V.; Credi, A.; Scandola, F. In *Transition Metals in Supramolecular Chemistry*; Fabbrizzi, L., Poggi, A., Eds.; Kluwer: Dordrecht, The Netherlands, 1994; p1. (c) Lehn, J.-M. *Supramolecular Chemistry—Concepts and Properties*; VCH: Weinheim, Germany, 1995. (d) Bignozzi, C. A.; Schoonover, J. R.; Scandola, F. *Prog. Inorg. Chem.* **1997**, *44*, 1.

(2) (a) Kalyanasundaran, K. *Coord. Chem. Rev.* **1982**, *46*, 159. (b) Chin, K.-F.; Cheung, K.-K.; Yip, H.-K.; Mak, T. C. W.; Che, C. M. *J. Chem. Soc., Dalton Trans.* **1995**, *4*, 657−665. (c) Sonoyama, N.; Karasawa, O.; Kaizu, Y. *J. Chem. Soc., Faraday Trans.* **1995**, *91*, 437. (d) Tan-Sien-Hee, L.; Mesmaeker, A. K.-D. *J. Chem. Soc., Dalton Trans.* **1994**, *24*, 3651−3658. (e) Kalyanasundaram, K.; Gratzel, M. *Coord. Chem. Rev.* **1998**, *177*, 347−414.

(3) (a) Anderson, P. A.; Anderson, R. F.; Furue, M.; Junk, P. C.; Keene, F. R.; Patterson, B. T.; Yeomans, B. D. *Inorg. Chem.* **2000**, *39*, 2721−2728. (b) Li, C.; Hoffman, M. Z. *Inorg. Chem.* **1998**, *37*, 830−832. (c) Berg-Brennan, C.; Subramanian, P.; Absi, M.; Stern, C.; Hupp, J. T. *Inorg. Chem.* **1996**, *35*, 3719−3722. (d) Kawanishi, Y.; Kitamura, N.; Tazuke, S. *Inorg. Chem.* **1989**, *28*, 2968−2975.

(4) (a) Balzani, V.; Juris, A.; Venturi, M.; Campagna, S.; Serroni, S. *Chem. Rev.* **1996**, *96*, 759. (b) Shaw, J. R.; Sadler, G. S.; Wacholtz, W. F.; Ryu, C. K.; Schmehl, R. H. *New J. Chem.* **1996**, *20*, 749.

(5) Dedeian, K.; Djurovich, P. I.; Garces, F. O.; Carlson, G.; Watts, R. J. *Inorg. Chem.* **1991**, *30*, 1685−1687.

(6) Colombo, M. G.; Brunold, T. C.; Riedener, T.; Güdel, H. U. *Inorg. Chem.* **1994**, *33*, 545−550.

(7) (a) Ohsawa, Y.; Sprouse, S.; King, K. A.; DeArmond, M. K.; Hanck, K. W.; Watts, R. J. *J. Phys. Chem.* **1987**, *91*, 1047−1058. (b) Wilde, A. P.; King, K. A.; Watts, R. J. *J. Phys. Chem.* **1991**, *95*, 629−634.

10.1021/ic0008969 CCC: $20.00
Published on Web 03/01/2001

nanosecond regime.[8] However, the Ir phosphor lifetimes are significantly shorter than phosphorescent lifetimes of common organic luminophores, which can range from many milliseconds to minutes (common for a spin-forbidden transition).[8] The significant decrease in the lifetime of the triplet excited state for the Ir complexes relative to the triplet excited state of organic molecules is a direct consequence of the strong spin−orbit coupling of the Ir center. The electronic transitions responsible for luminescence in these cyclometalated complexes have been assigned to mixture of MLCT and ligand-centered transitions.[7b,9] An interesting application for these organometallic Ir complexes is their use as phosphors in organic light emitting diodes (OLEDs). The excited states generated in electroluminescence are trapped at the phosphor, where strong spin−orbit coupling leads to efficient phosphorescence at room temperature and efficient utilization of these excited states.[10] OLEDs prepared with these heavy metal complexes are the most efficient OLEDs reported to date,[10] with efficiencies of greater than 80% (photons/electrons) reported for Ir(*ppy*)$_3$ based OLEDs.[11]

Unfortunately, many of the cyclometalating ligands that could be incorporated into Ir-based phosphors do not give tris-ligand complexes by the reported synthetic methods. Herein we describe the synthesis as well as spectroscopic and structural characterization of a class of highly phosphorescent Ir complexes. These complexes have two cyclometalated ligands and a single bidentate, monoanionic ancillary ligand, making the complexes neutral and sublimable. The emission color from the complex is dependent on the choice of cyclometalating ligand, ranging from green to red. The structures of two of these complexes have been determined and strongly resemble that of the chloride-bridged dimers prepared with the same cyclometalated ligands, i.e., $\underline{C\wedge N}_2$Ir(μ-Cl)$_2$Ir$\underline{C\wedge N}_2$.

Experimental Section

UV−visible spectra were measured on an Aviv model 14DS spectrophotometer (a re-engineered Cary 14 spectrophotometer). Photoluminescent spectra were measured with a Photon Technology International fluorimeter. Quantum efficiency measurements were carried out at room temperature in a 2-MeTHF solution (degassed by several freeze−pump−thaw cycles). Degassed solutions of *fac*-Ir(*ppy*)$_3$ were used as a reference. Steady state emission experiments at room temperature were performed on a PTI QuantaMaster model C-60 spectrofluorimeter. Phosphorescence lifetime measurements were performed on the same fluorimeter equipped with a microsecond Xe flash lamp. NMR spectra were recorded on Bruker AC 250 MHz, AM 360 MHz, or AMX 500 MHz instruments. Solid probe MS spectra were taken with Hewlett-Packard GC/MS instrument with electron impact ionization and model 5873 mass sensitive detector. High-resolution mass spectrometry was done at Frick Chemical Laboratory at Princeton University. The Microanalysis Laboratory at the University of Illinois, Urbana-Campaign, performed all elemental analyses.

All procedures involving IrCl$_3$·H$_2$O or any other Ir(III) species were carried out in inert gas atmosphere despite the air stability of the compounds, the main concern being their oxidative and thermal stability of intermediate complexes at the high temperatures used in the reactions. Cyclometalated Ir(III) μ-chloro-bridged dimers of general formula $\underline{C\wedge N}_2$Ir(μ-Cl)$\underline{IrC\wedge N}_2$ were synthesized by the method reported by Nonoyama, which involves refluxing IrCl$_3$·*n*H$_2$O (Next Chimica) with 2−2.5 equiv of cyclometalating ligand in a 3:1 mixture of 2-methoxyethanol (Aldrich Sigma) and water.[15]

Synthesis of (<ul;1>*C*∧*N*)$_2$Ir(acac) Complexes. General Procedure. [($\underline{C\wedge N}$)$_2$IrCl]$_2$ complex (0.078 mmol), 0.2 mmol of 2,4-pentanedione (Aldrich Sigma), and 85−90 mg of sodium carbonate were refluxed under inert gas atmosphere in 2-ethoxyethanol for 12−15 h. After cooling to room temperature, the colored precipitate was filtered off and was washed with water, followed by 2 portions of ether and hexane. The crude product was flash chromatographed using a silica/dichloromethane column to yield ca. 75−90% of the pure ($\underline{C\wedge N}$)$_2$Ir(acac) after solvent evaporation and drying.

(*ppy*)$_2$Ir(acac): iridium(III) bis(2-phenylpyridinato-*N*,*C*$^{2'}$) acetylacetonate (yield 83%). ^{1}H NMR (360 MHz, acetone-d_6), ppm: 8.55 (d, 2H, J 5.8 Hz), 8.07 (d, 2H, J 7.9 Hz), 7.91 (t, 2H, J 7.4 Hz), 7.63 (d, 2H, J 7.9 Hz), 7.32 (t, 2H, J 7.4 Hz), 6.74 (t, 2H, J 7.4 Hz), 6.59 (t, 2H,J 5.8 Hz), 6.21 (d, 2H, *J* 7.4 Hz), 5.26 (s, 1H), 1.69 (s, 6H). Anal. Found: C 54.20, H 3.92, N 4.71. Calcd: C 54.08, H3.87, N4.67.

(*tpy*)$_2$Ir(acac): iridium(III) bis(2-(4-tolyl)pyridinato-*N*,*C*$^{2'}$) acetylacetonate (yield 75%). ^{1}H NMR (500 MHz, CDCl$_3$), δ, ppm: 8.45 (d, 2H, J 5.1 Hz), 7.77 (d, 2H, J 8.3 Hz), 7.68 (dt, 2H, 7.4, 1.4 Hz), 7.42 (d, 2H, J 8.3 Hz), 7.07 (ddd, 2H, J 6.9, 6.5, 1.4 Hz), 6.61 (d, 2H, J 7.8 Hz), 6.04 (s, 2H), 5.17 (s, 1H), 1.54 (s, 6H). Anal. Found: C 55.35, H 4.40, N 4.52. Calcd: C 55.49, H 4.43, N 4.46.

(*bzq*)$_2$Ir(acac): iridium(III) bis(7,8-benzoquinolinato-*N*,*C*$^{3'}$) acetylacetonate (yield 90%). ^{1}H NMR (360 MHz, acetone-d_6), ppm: 8.96 (d, 2H, J 4.8 Hz), 8.49 (d, 2H, J 7.9 Hz), 7.80 (6H,6,8, m), 7.26 (d, 2H, J 7.9 Hz), 6.89 (t, 2H, J 7.4 Hz), 6.21 (t, 2H, J 7.9 Hz), 5.33 (s, 1H), 1.69 (s, 6H). Anal. Found: C 58.15, H 3.89, N 4.37. Calcd: C 58.08, H 3.81, N 4.23.

(*bt*)$_2$Ir(acac): iridium(III) bis(2-phenylbenzothiozolato-*N*,*C*$^{2'}$) acetylacetonate. ^{1}H NMR (360 MHz, DMSO-d_6), ppm: 8.25 (m, 2H), 7.93 (m, 2H), 7.74 (dd, 2H, J 8.0, 2.0 Hz), 7.55 (m, 4H), 6.85 (td, 2H, J 7.6, 1.0 Hz), 6.60 (td, 2H, J 7.6, 1.0 Hz), 6.20 (dt, 2H, 7.5, 0.6 Hz), 5.12 (s, 1H), 1.71 (s, 6H). Anal. Found: C 52.08, H 3.30, N 3.47. Calcd: C 52.23, H 3.39, N 3.93.

(*bt*)$_2$Ir(pico): iridium(III) bis(2-phenylbenzothiozolato-*N*,*C*$^{2'}$) picolinate. ^{1}H NMR (360 MHz, DMSO-d_6), ppm: 8.24 (m, 3H), 8.09 (td, 1H, J 7.5, 1.7 Hz), 7.99 (d, 1H, J 7.7 Hz), 7.91 (dd, 1H, J 7.8, 0.8 Hz), 7.83 (m, 2H), 7.70 (m, 1H), 7.49 (m, 2H), 7.43 (t, 1H, J 4.5 Hz), 7.13 (t, 1H, J 7.9 Hz), 7.00 (td, 1H, J 7.7, 1.0 Hz), 6.95 (td, 1H, J 7.3, 1.2 Hz), 6.78 (td, 1H, J 7.3, 0.9 Hz), 6.73 (td, 1H, J 7.5, 1.2 Hz), 6.41 (d, 2H, J 7.7 Hz), 6.15 (d, 1H, J 7.7 Hz), 6.00 (d, 1H, J 8.3 Hz). Anal. Found: C 52.44, H 2.72, N 5.35. Calcd: C 52.30, H 2.74, N 5.72.

(*bt*)$_2$Ir(sal): iridium(III) bis(2-phenylbenzothiozolato-*N*,*C*$^{2'}$) (*N*-methylsalicylimine-*N*,*O*). ^{1}H NMR (360 MHz, acetone-d_6), ppm: 8.60 (d, 1H, J 8.4 Hz), 8.15 (d, 1H, J 8.4 Hz), 8.09 (m, 1H), 7.86 (d, 1H, J 8.0 Hz), 7.78 (d, 1H, J 7.6 Hz), 7.70 (d, 1H, J 7.6 Hz), 7.41−7.52 (m, 3H), 7.31 (t, 1H, J 8.4 Hz), 6.99−7.05 (m, 2H), 6.83−6.89 (m, 2H), 6.61−6.67 (m, 2H), 6.43−6.49 (m, 2H), 6.27 (d, 1H, J 7.6 Hz), 6.18 (t, 1H, J 7.6 Hz), 5.61 (s, 1H), 3.13 (s, 3H). Anal. Found: C 53.62, H 3.44, N 4.85. Calcd: C 54.67, H 3.24, N 5.63.

(*bsn*)$_2$Ir(acac): iridium(III) bis(2-(1-naphthyl)benzothiazolato-*N*,*C*$^{2'}$) acetylacetonate. ^{1}H NMR (250 MHz, CDCl$_3$), ppm: 8.56 (d, 2H, J 7.8 Hz), 8.09 (d, 2H, J 7.9 Hz), 7.99 (d, 2H, J 7.5 Hz), 7.60 (m, 4H), 7.43 (m, 4H), 7.31 (t, 2H, J 7.8 Hz), 6.99 (d, 2H, J 8.2 Hz), 6.55 (d, 2H, J 8.5 Hz), 5.07 (s, 1H), 1.72 (s, 6H). Anal. Found: C 57.69, H 3.35, N 3.45. Calcd: C 56.56, H 3.51, N 3.03.

(*pq*)$_2$Ir(acac): iridium(III) bis(2-phenylquinolyl-*N*,*C*$^{2'}$) acetylacetonate (yield ca. 95%). ^{1}H NMR (360 MHz, DMSO-d_6), ppm: 8.51 (d, 2H, 8 Hz), 8.37 (m, 4H), 8.01 (m, 4H), 7.55 (m, 4H), 6.88 (tm, 2H, 5

(8) Turro, N. J. *Modern Molecular Photochemistry*; The Benjamin/Cummings Publishing Co., Inc.; Menlo Park, California, 1978. Murov, S. L.; Carmichael, I.; Hug, G. L. *Handbook of Photochemistry*; Marcel Dekker: New York, 1993.
(9) (a) Sprouse, S.; King, K. A.; Spellane, P. J.; Watts, R. J. *J. Am. Chem. Soc.* **1984**, *106*, 6647−6653. (b) Crosby, G. A. *J. Chim. Phys.* **1967**, *64*, 160.
(10) (a) Baldo, M. A.; O'Brien, D. F.; You, Y.; Shoustikov, A.; Sibley, S.; Thompson, M. E.; Forrest, S. R. *Nature* **1998**, *395*, 151. (b) Baldo, M. A.; Lamansky, S.; Burrows, P. E.; Thompson, M. E.; Forrest, S. R. *Appl. Phys. Lett.* **1999**, *75*, 4. (c) Thompson, M. E.; Burrows, P. E.; Forrest, S. R. *Curr. Opin. Solid State Mater. Sci.* **1999**, *4*, 369.
(11) Adachi, C.; Forrest, S. R.; Thompson, M. E. *Appl. Phys. Lett.*, in press.
(12) XSCANS system of data collection solution software: Siemens Analytical Instruments, Madison, Wisconsin.
(13) G. M. Sheldrick, SHELX system of programs for crystallographic analysis, University of Göttingen, Germany.
(14) Program DIFABS for empirical absorption corrections: Walker, N.; Stuart, D. *Acta Crystallogr.* **1983**, *A39*, 158.
(15) Nonoyama, M. *Bull. Chem. Soc. Jpn.* **1974**, *47*, 767.

Hz), 6.53 (td, 2H, 7 Hz, 1 Hz), 6.29 (dd, 2H, 8 Hz, 1 Hz), 4.70 (s, 1H), 2.08 (s, 6H).

***fac*-Ir(ppy)$_3$:** iridium(III) *fac*-tris(2-phenylpyridinato-*N*,$C^{2'}$). Iridium(III) bis(2-phenylpyridinato-*N*,$C^{2'}$) acetylacetonate (0.20 mmol) and phenylpyridine (0.5 mmol) were refluxed for 15 h in 10 mL of glycerol to give a yellow suspension upon cooling. The crude product was isolated by filtration, washed with hexane and ether, dried in a vacuum, and zone sublimed (sample sublimed in a temperature gradient of 300−270 °C) to give a green-yellow product (yield 85%). Analytical data matches that reported for *fac*-Ir(*ppy*)$_3$.[5]

Ir(*bzq*)$_3$: iridium(III) *fac*-tris(7,8-benzoquinolinate-*N*,$C^{3'}$). This complex was prepared by two different methods, method A and method B.

Method A. This complex was prepared from Ir(acac)$_3$ by a procedure analogous to the one reported for Ir(*ppy*)$_3$.[5] Ir(acac)$_3$ (50 mg) and 7,8-benzoquinoline (113 mg) were dissolved in 5 mL of glycerol and refluxed for 12−15 h under an inert atmosphere. After cooling, the product was filtered off and washed with several 10 mL portions of hexanes, ether, and acetone. The crude product was sublimed to give a 32% yield of orange Ir(*bzq*)$_3$.The Ir(*bzq*)$_3$ product from this reaction is a mixture of *fac*- and *mer*-isomers. Several wash cycles (acetone and dichloromethane) cause significant enrichment of the mixture in *fac*-product but still does not allow isolation of a pure *facial* complex. ^{1}H NMR (500 MHz, CD_2Cl_2), ppm: 8.31 (d, J 8.1 Hz), 8.19 (d, J 8.0 Hz), 8.12 (d, J 10.0 Hz), 8.03 (m), 7.9 (m), 7.6 (m), 7,47 (t, J 7.5 Hz), 7.39 (t, J 7.4 Hz), 7.22 (m), 7.14 (m), 7.07 (m), 6.96 (d, J 8.0 Hz), 6.80 (d, J 8.1 Hz), 6.57 (d, J 7.9 Hz). Anal. Found: C 63.55, H 3.51, N 5.32. Calcd: C 64.45, H 3.33, N 5.78.

Method B. (*bzq*)$_2$Ir(acac) (0.16 mmol) and 7,8-benzoquinoline (0.5 mmol) were refluxed for 15 h in 10 mL of glycerol to give a yellow-orange suspension upon cooling. The crude product was isolated by filtration, washed with hexane and ether, dried in a vacuum, and zone sublimed (sample sublimed in a temperature gradient of 300−270 °C) to give an orange product, a mixture of *fac*- and *mer*-isomers (total yield 75%). ^{1}H NMR and elemental analysis characterization match those listed for Ir(*bzq*)$_3$ prepared by method A.

Electrochemistry. Cyclic voltammograms (CV) were recorded on an EG&G potentiostat/galvanostat model 283 in degassed dichloromethane solutions using 0.1 M tetra(*n*-butyl)ammonium hexafluorophosphate as a supporting electrolyte and a Ag/AgCl reference electrode. The Cp_2Fe/Cp_2Fe^+ redox couple was used as a secondary, internal reference. All studied complexes showed reversible oxidation waves with half-wave potentials of 870, 820, 860, 930, and 1000 mV for (*ppy*)$_2$Ir(acac), (*tpy*)$_2$Ir(acac), (*bzq*)$_2$Ir(acac), (*bsn*)$_2$Ir(acac), and (*bt*)$_2$Ir(acac) vs Ag/AgCl, respectively.

Crystallography. Diffraction data for (*tpy*)$_2$Ir(acac) and (*ppy*)$_2$Ir(acac) were collected at $T = -100$ °C on a Siemens P4 diffractometer with Mo Kα radiation ($\lambda = 0.71073$ A). The cell dimensions and orientation matrix for data collection were obtained from a least-squares refinement of the setting angles of at least 25 accurately centered reflections. Data collection in the 2θ scan mode, cell refinement, and data reduction were carried out with the use of the program XSCANS[12] and resulted in data sets of 2176 reflections for (*ppy*)$_2$Ir(acac) and 4663 reflections for (*tpy*)$_2$Ir(acac). Pertinent crystal and unit cell parameters are given in Table 1. The (*ppy*)$_2$Ir(acac) crystal used in the X-ray diffraction study was of lower quality than the (*tpy*)$_2$Ir(acac) crystal. We attempted to grow better crystals of (*ppy*)$_2$Ir(acac), but could not get better crystals than the one used here. As a result the (*ppy*)$_2$Ir(acac) crystal only gave useful data out to $2\theta = 45°$, while the (*tpy*)$_2$Ir(acac) diffracted strongly to well beyond the 50° cutoff used here. The lower quality of the (*ppy*)$_2$Ir(acac) crystal is reflected in the comparatively higher *R* factor for the (*ppy*)$_2$Ir(acac) structure.

The structures were solved by direct methods using the SHELXS[13] package of computer programs. Both structures were refined by full-matrix least-squares methods based on F^2 using SHELX93[13] and corrected for absorption by the program DIFABS.[14] Calculated hydrogen positions were input and refined in a riding manner along with their attached carbons. Due to the limited data set for (*ppy*)$_2$Ir(acac), the Ir was refined anisotropically and all other atom positions were refined isotropically. For (*tpy*)$_2$Ir(acac), the non-hydrogen atom positions were refined anisotropically and the hydrogen positions were refined isotropically. A summary of the refinement details and the resulting agreement factors is given in Table 1. In both cases the Ir centers are octahedrally coordinated by the three chelating ligands, with the N atoms in a trans configuration, and a 2-fold rotation axis passes through the Ir atom and the acac ligand.

Table 1. Crystal Data and Summary of Intensity Data Collection and Structure Refinement

	(*ppy*)$_2$Ir(acac)	(*tpy*)$_2$Ir(acac)
empirical formula	$C_{27}H_{23}IrN_2O_2$	$C_{29}H_{26}IrN_2O_2$
fw	599.67	626.72
temp, K	173	173
wavelength, Å	0.71073	0.71073
cryst syst	orthorhombic	triclinic
space group	*Pbcn* (No. 60)	$P\bar{1}$ (No. 2)
unit cell dimens		
a (Å)	13.171(3)	9.697(2)
b (Å)	10.086(3)	11.616(1)
c (Å)	16.613(3)	12.371(1)
α (deg)	90	64.340(6)
β (deg)	90	76.153(9)
γ (deg)	90	87.211(10)
vol, Å^3	2206.9(8)	1217.2(4)
Z	4	2
density (calcd), g/cm^3	1.805	1.710
abs coeff, mm^{-1}	6.08	5.51
F(000)	1168	614
θ range for data collection, deg	2.5−22.5	2.0−25.0
index ranges	$0 \le h \le 14$, $0 \le k \le 10$, $0 \le l \le 17$	$-9 \le h \le 9$, $-12 \le k \le 12$, $0 \le l \le 14$
reflns collected	2176	4663
indep reflns	1410 [*R*(int) = 0.074]	3745 [*R*(int) = 0.0233]
refinement meth	full-matrix least-squares on F^2	full-matrix least-squares on F^2
data/restraints/params	1409/0/71	3745/0/309
GOF on F^2	1.129	0.725
final *R* index [$I > 2\sigma(I)$]	0.0678	0.0270
R index (all data)	0.0870	0.0336

Results and Discussion

Synthesis and Characterization of $\underline{C\wedge N}_2$Ir(LX) Complexes. Iridium chloride reacts with phenylpyridine in refluxing 2-ethoxyethanol to give a cyclometalated complex.[15] The product of this reaction is a chloride-bridged dimer, (*ppy*)$_2$Ir(*μ*-Cl)$_2$Ir(*ppy*)$_2$, *ppy* = 2-phenylpyridinato-C^2,*N*, eq 1. This cyclometalation reaction leads to a similar chloride-bridged dimer for other substituted pyridyl or heterocyclic ligands as well, i.e., 2-phenylbenzothiazole (*bt*), benzoquinoline (*bzq*), and donor- or acceptor-substituted phenylpyridines.[9b,16] Crystallographic studies of the *ppy* complex show that the Ir center in (*ppy*)$_2$Ir(*μ*-Cl)$_2$Ir(*ppy*)$_2$ is octahedrally coordinated by the two bridging chlorides and two cyclometalated *ppy* ligands, with the heterocyclic rings of the ligands in a trans configuration,[16a,17] as illustrated in Figure 1b. Crystal structures have not been reported for the other chloride-bridged dimers, but NMR data suggests a structure similar to that of (*ppy*)$_2$Ir(*μ*-Cl)$_2$Ir(*ppy*)$_2$.[16b,18]

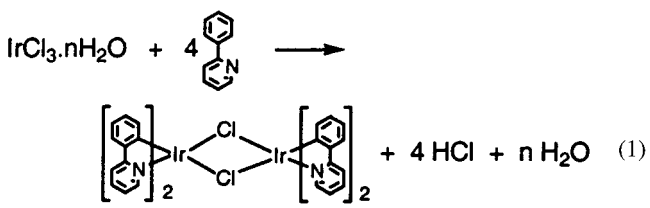

(1)

We have found this cyclometalation reaction to be a general one, giving good yields of the corresponding $\underline{C\wedge N}_2$Ir(*μ*-

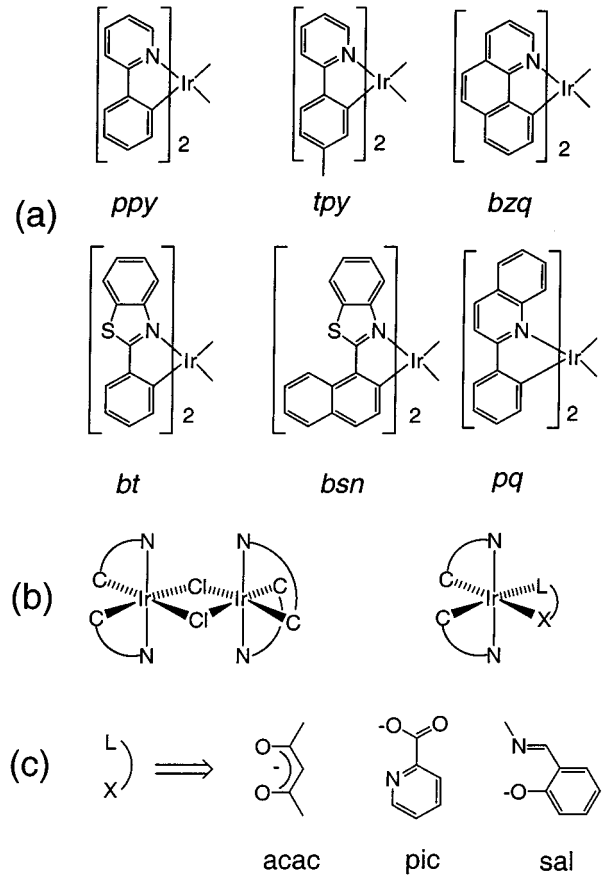

Figure 1. $\underline{C\wedge N}_2$Ir(LX) complexes. The $\underline{C\wedge N}_2$Ir fragments are shown in part a, with the acronym used for each $\underline{C\wedge N}$ ligand listed under the fragment. The coordination geometries of $\underline{C\wedge N}_2$Ir(μ-Cl)$_2$Ir$\underline{C\wedge N}_2$ and $\underline{C\wedge N}_2$Ir(acac) complexes are shown in part b. The identities of the LX ligands are shown in part c.

Cl)$_2$Ir$\underline{C\wedge N}_2$ dimers ($\underline{C\wedge N}$ = cyclometalated ligand) for a number of ligands. The ligands examined here are shown in Figure 1. The reactions to form the dimers proceed under fairly mild conditions, giving good yields of the organometallic complexes, typically greater than 75%. All of the ligands used here have a heterocyclic nitrogen and an sp^2-hybridized carbon positioned such that the cyclometalation reaction leads to a five-membered ring. The NMR spectra of these complexes are consistent with the heterocyclic rings of the C,N ligands being in a trans disposition, as shown in Figure 1b. The chloride-bridged complexes form a racemic mixture of $\Delta\Delta/\Lambda\Lambda$ dimers that are characterized by pronounced downfield shifts in the ^{1}H NMR resonance of heterocyclic protons nearest to the bridging chlorides.[19]

$\underline{C\wedge N}_2$Ir(μ-Cl)$_2$Ir$\underline{C\wedge N}_2$ complexes show strong MLCT- and ligand-based absorption bands. These dimers are not strongly emissive at room temperature; however, they phosphoresce strongly in frozen glasses at 77 K. When the dimer is dissociated into monomeric Ir complexes, either by preparing an Ir$\underline{C\wedge N}_3$ complex or a cationic species, e.g., (*ppy*)$_2$Ir(bpy)$^+$ (bpy = 2,2′-bipyridine), the phosphorescence efficiency increases markedly. The weak phosphorescence of the chloride-bridged dimers has been attributed to a monomer−dimer equilibrium that occurs in solution.[16c] The tris-chelate complexes are attractive in a number of applications due to their high phosphorescence efficiencies and microsecond lifetimes; however, we have found it very difficult to make the complexes for many of the cyclometalated ligands of interest. While we were able to prepare the chloride-bridged dimers for all of the $\underline{C\wedge N}$ ligands shown in Figure 1, the preparation of tris-chelates, i.e., Ir$\underline{C\wedge N}_3$, has only been possible for *ppy*, *tpy*, and *bzq* ligands.

The chloride-bridged dimers can be converted to emissive, monomeric complexes by treating the dimer with a bidentate, anionic ancillary ligand (LX), such as a β-diketonate, 2-picolinic acid, or an *N*-alkylsalicylimine, eq 2. These reactions give $\underline{C\wedge N}_2$-Ir(LX) in high yield, typically greater than 80%. The majority of the $\underline{C\wedge N}_2$Ir(LX) complexes prepared are emissive at room temperature, with λ_{max} values between 510 and 610 nm, Table 2. The complexes are stable in air and can be sublimed in a vacuum without decomposition.

$$\underline{C\wedge N}_2\text{Ir}(\mu\text{-Cl})_2\text{Ir}\underline{C\wedge N}_2 + 2\text{LXH} \rightarrow \underline{C\wedge N}_2\text{Ir(LX)} + 2\text{HCl} \quad (2)$$

Analysis by cyclic voltammetry shows that the $\underline{C\wedge N}_2$Ir(acac) complexes all undergo a reversible one-electron oxidation; however, no reduction processes were observed in CH_2Cl_2. The oxidation potentials of these complexes vary between 0.8 and 1.0 V (vs Ag/AgCl), Table 2. The complexes with pyridyl type ligands (i.e., *ppy*, *tpy*, and *bzq*) are easier to oxidize than the complexes with benzothiazolyl based ligands (i.e., *bt* and *bsn*). The oxidation potentials of (*ppy*)$_2$Ir(acac) and (*tpy*)$_2$Ir(acac) are ca. 300 mV less positive than the values reported for the corresponding cationic (*ppy*)$_2$Ir(L′)$^+$ and (*tpy*)$_2$Ir(L′)$^+$ complexes, where L′ = 2,2′-bipyridine or 1,10-phenanthroline.[7a,16a] The oxidation potentials of the *ppy* and *tpy* complexes are comparable to those found in Ir$\underline{C\wedge N}_3$ complexes with the same ligands, showing that the metal-localized HOMOs are at very similar energies.

The $\underline{C\wedge N}_2$Ir(acac) complexes can be used to prepare Ir$\underline{C\wedge N}_3$. Treating (*ppy*)$_2$Ir(acac) with phenylpyridine in refluxing glycerol gives Ir(*ppy*)$_3$ in greater than 75% yield. The overall yield of Ir(*ppy*)$_3$ (based on $IrCl_3 \cdot n H_2O$) by this route is greater than 60%, compared to less than 20% when Ir(acac)$_3$ is used as the intermediate.[20] Similar yields have been achieved for the synthesis of Ir(*bzq*)$_3$ and Ir(2-(2-thienyl)pyridine)$_3$ via the $\underline{C\wedge N}_2$-Ir(acac) complexes. Only $\underline{C\wedge N}_2$Ir(acac) complexes of phenylpyridines, benzoquinoline, and thienylpyridine form tris complexes when reacted with excess $\underline{C\wedge N}$ ligand. To the best of our knowledge this is the first report of a tris-cyclometalated complex of benzoquinoline, Ir(*bzq*)$_3$. Based on molecular modeling there are no obvious steric interactions that would prevent the formation tris complexes from *bt*, *bsn*, or *pq* ligands. However, other factors such as imine basicity could play a controlling role in stabilizing intermediates in the mechanism of tris complex formation.

Photophysical Properties of $\underline{C\wedge N}_2$Ir(acac) Compounds. The absorption spectra for (*tpy*)$_2$Ir(acac) and (*bzq*)$_2$Ir(acac) are characteristic of $\underline{C\wedge N}_2$Ir(LX) complexes, Figure 2. Intense bands are observed in the ultraviolet part of the spectra, between 250 and 350 nm, which can be assigned to the allowed $^1(\pi-\pi^*)$

(16) (a) Garces, F. O.; King, K. A.; Watts, R. J. *Inorg. Chem.* **1988**, *27*, 3464−3471. (b) Carlson, G. A.; Djurovich, P. I.; Watts, R. J *Inorg. Chem.* **1993**, *32*, 4483−4484.
(17) Garces, F. O.; Dedian, K.; Keder, N. L.; Watts, R. J. *Acta Crystallogr.* **1993**, *C49*, 1117.
(18) (a) Yin, C. C.; Deeming, A. J. *J. Chem. Soc., Dalton Trans.* **1975**, 2091. (b) Nord, G.; Hazell, A. C.; Hazell, R. G.; Farver, O. *Inorg. Chem.* **1983**, *22*, 3429−3434. (c) Spellane, P. J.; Watts, R. J.; Curtis, C. J. *Inorg. Chem.* **1983**, *22*, 4060−4062.
(19) Garces, F. O.; Watts, R. J. *J. Magn. Reson. Chem.* **1993**, *31*, 529.
(20) The reported yield of Ir(acac)$_3$ from $IrCl_3 \cdot n H_2O$ is 35% (Collins, J. E.; Castellani, M. P.; Rheingold, A. L.; Miller, E. J.; Geiger, W. E.; Rieger, A. L.; Rieger, P. H. *Organometallics* **1995**, *14*, 1232−1238), and the yield of Ir$\underline{C\wedge N}_3$ from Ir(acac)$_3$ is 40%.[5]

Table 2. Photophysical and Electrochemical Data for $\underline{C\wedge N}_2$Ir(LX) Complexes

$\underline{C\wedge N}$	LX	absorbance λ (log ϵ)	emission λ_{max} (nm)	lifetime (μsec)[a] 77 K	lifetime (μsec)[a] 298 K	quantum efficiency*	oxidation potential mV vs Ag/AgCl
ppy	acac	260 (4.5), 345 (3.8), 412 (3.4), 460 (3.3), 497 (3.0)	516	3.2	1.6	0.34	870
tpy	acac	270 (4.5), 370 (3.7), 410 (3.5), 460 (3.4), 495 (3.0)	512	4.5	3.1	0.31	820
bzq	acac	260 (4.6), 360 (3.9), 470 (3.3), 500 (3.2)	548	23.3	4.5	0.27	860
bt	acac	269 (4.6), 313 (4.4), 327 (4.5), 408 (3.8), 447 (3.8), 493 (3.4), 540 (3.0)	557	4.4	1.8	0.26	1000
bt	pic	206 (4.6), 326 (4.6), 355 (4.1), 388 (3.9), 437 (3.8), 475 (3.7)	541	3.6	2.3	0.37	
bt	sal	276 (4.6), 325 (4.3), 450 (3.7), 540 (2.9)	562	3.1	1.4	0.22	
bsn	acac	274 (4.7), 300 (4.6), 345 (4.5), 427 (4.0), 476 (4.0), 506 (3.9)	606	2.5	1.8	0.22	930
pq	acac	268 (5.0), 349 (4.4), 433 (3.9), 467 (3.9), 553 (3.6)	597		2.0	0.10	

[a] Lifetime and quantum efficiency measurements were made in 2-MeTHF, except for the 77 K lifetime of $(ppy)_2$Ir(acac), which was carried out in a CH_2Cl_2 frozen glass. The lifetimes have error bars of ±10%, and the quantum efficiencies are ±20%.

transitions of the $\underline{C\wedge N}$ ligands. The energies and extinction coefficients for these bands correlate well with the transitions observed for the free hydrocarbons, i.e., tolylpyridine and benzoquinoline.[6,16] Somewhat weaker bands are observed at lower energies (λ_{max} > 400 nm). In other cyclometalated complexes these bands have been assigned to singlet and triplet MLCT transitions, and the same assignment is likely here.[6,16] In the spectra for $(tpy)_2$Ir(acac), two MLCT bands are clearly resolved at 410 and 460 nm, with extinction coefficients of 3500 and 2500 M^{-1} cm^{-1}, respectively. The formally spin forbidden ^{3}MLCT at 460 nm gains intensity by mixing with the higher lying ^{1}MLCT transition through the strong spin−orbit coupling of Ir. This mixing is strong enough in these Ir complexes that the formally spin forbidden ^{3}MLCT has an extinction coefficient that is more than half that of the spin-allowed ^{1}MLCT. In some cases, the ^{1}MLCT and ^{3}MLCT are not clearly resolved, as seen in $(bzq)_2$Ir(acac), where a broad band is observed between 430 and 520 nm. The spectra observed for $\underline{C\wedge N}_2$Ir(LX) complexes are very similar to those of the $\underline{C\wedge N}_2$Ir(μ-Cl)$_2$Ir $\underline{C\wedge N}_2$ and $\underline{C\wedge N}_2$Ir(bpy)$^+$ complexes with the same $\underline{C\wedge N}$ ligand,[7a,16b] suggesting that the dominant absorptions in the $\underline{C\wedge N}_2$Ir(LX) are due to the "$\underline{C\wedge N}_2$Ir" fragment, which has the same structure in all three types of complexes, *vide infra*.

All of the $\underline{C\wedge N}_2$Ir(LX) complexes reported here give phosphorescence quantum yields between 0.1 and 0.4, and luminescence lifetimes between 1 and 5 μs for degassed solutions at room temperature, Figure 2. These photophysical parameters are very similar to those of the *fac*-Ir$\underline{C\wedge N}_3$ complexes. The emission spectra of the $\underline{C\wedge N}_2$Ir(acac) complexes match those of the *fac*-Ir$\underline{C\wedge N}_3$ complexes prepared with the same C∧N ligands for *ppy*-, *tpy*-, and *bzq*-based complexes, Figure 2. It has been shown that emission from Ir$(ppy)_3$ comes from MLCT transitions.[6,21] Considering that the absorption spectra of the *ppy* and *bzq* complexes reported here are very similar to their Ir$\underline{C\wedge N}_3$ and $\underline{C\wedge N}_2$Ir(L′)$^+$ analogues, it is not surprising that the emission spectra of $\underline{C\wedge N}_2$Ir(acac) and Ir$\underline{C\wedge N}_3$ complexes are similar, since all of the *ppy*, *tpy*, and *bzq* complexes presumably emit from MLCT states of the same energy.

Changes in the $\underline{C\wedge N}$ligand in a $\underline{C\wedge N}_2$Ir(LX) complex typically have a marked effect on the phosphorescence spectrum, while changing the LX ligand leads to a relatively minor shift.

Table 3. Selected Bond Distances (Å) and Angles (deg) for $(ppy)_2$Ir(acac) and $(tpy)_2$Ir(acac)

	$(ppy)_2$Ir(acac)	$(tpy)_2$Ir(acac)
Bond Distances (Å)		
Ir(1)−N(1)	2.010(9)	2.040(5)
Ir(1)−N(1)*/Ir(1)−N(2)	2.010(9)	2.023(5)
Ir(1)−C(11)/Ir(1)−C(12)	2.003(9)	1.985(7)
Ir(1)−C(11)*/Ir(1)−C(24)	2.003(9)	1.982(6)
Ir(1)−O(1)/Ir(1)−O(2)	2.146(6)	2.161(4)
Ir(1)−O(1)*/Ir(1)−O(1)	2.146(6)	2.136(4)
Angles (deg)		
N(1)−Ir(1)−N(1)*/N(1)−Ir(1)−N(2)	176.3(4)	176.2(2)
N(1)−Ir(1)−C(11)/N(1)−Ir(1)−C(12)	81.7(4)	80.4(2)
N(1)*−Ir(1)−C(11)*/N(2)−Ir(1)−C(24)	81.7(4)	80.3(2)
N(1)−Ir(1)−O(1) /N(1)−Ir(1)−O(2)	94.5(3)	94.2(2)
C(11)*−Ir(1)− O(1) /C(24)−Ir(1)− O(2)	87.5(3)	91.3(2)
O(1)−Ir(1)−O(1)* /O(12)−Ir(1)−O(1)	90.0(3)	88.2(2)

ppy and *tpy* ligands give green emission, *bzq* and *bt* ligands give yellow emission, *pq* ligands give orange emission, and the *bsn* complex gives red emission. If the pyridyl group of *ppy* is replaced with a 2-quinolinyl group, the emission line is shifted by 77 nm. A similar red shift is observed if the phenyl group of the *bt* ligand is replaced with an α-naphthyl group (*bsn*). The spectra of $\underline{C\wedge N}_2$Ir(LX) complexes show very little LX ligand character in the excited state. For example, $(bt)_2$Ir(LX) (LX = acac, pic, and sal) give very similar spectra, Figure 2c, with only minor shifts as a function of the LX ligand. Vibronic fine structure is observed in the $(bt)_2$Ir(LX) emission spectra, consistent with a significant ligand $^3(\pi-\pi^*)$ contribution to the phosphorescence, as observed in related Ir$\underline{C\wedge N}_3$ complexes.[6]

Structures of $\underline{C\wedge N}_2$Ir(LX) Complexes. Molecular plots of $(ppy)_2$Ir(acac) and $(tpy)_2$Ir(acac) are shown in Figure 3a and Figure 3b, respectively. Crystallographic data are given in Table 1, and selected bond lengths (Å) and angles (deg) for these complexes are presented in the Table 3. Crystals of $(ppy)_2$Ir(acac) were of lower quality than those of $(tpy)_2$Ir(acac), which is reflected in the poorer agreement factor for the $(ppy)_2$Ir(acac) complex. The molecular structures and solid state packing determined for the two complexes are very similar. The *tpy* and *ppy* complexes have an octahedral coordination geometry around Ir, retaining the *cis*-C,C *trans*-N,N chelate disposition of the chloride-bridged precursor complex, i.e., $(tpy)_2$Ir(μ-Cl)$_2$Ir$(tpy)_2$. The Ir−C bonds of these complexes (Ir−C_{av} = 1.993(8) Å) are shorter than the Ir−N bonds (Ir−N_{av} = 2.021(7) Å). These Ir−C bond lengths are similar to values of 2.02(2)−2.13(6) Å reported for the $(tpy)_2$Ir(μ-Cl)$_2$Ir$(tpy)_2$ and *fac*-Ir$(tpy)_3$[17] com-

(21) Colombo, M. G.; Hauser, A.; Güdel, H. U. *Inorg. Chem.* **1993**, *32*, 3088−3092.

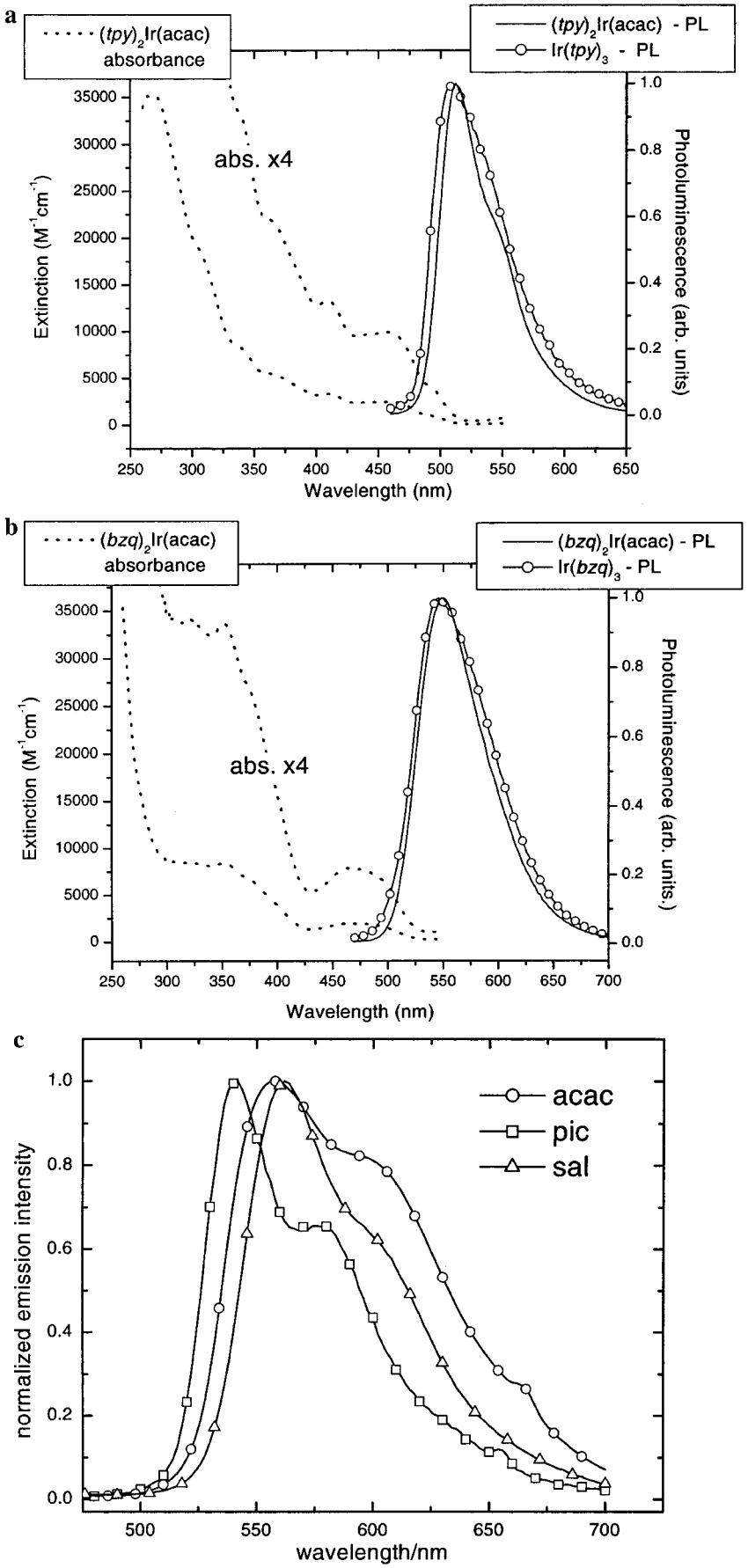

Figure 2. Absorption spectra for $\underline{C\wedge N}_2$Ir(LX) and photoluminescence spectra for $\underline{C\wedge N}_2$Ir(LX) and Ir$\underline{C\wedge N}_3$ complexes. Spectra for $(tpy)_2$Ir(acac) and *fac*-Ir$(ppy)_3$ are shown in part a. The absorption and emission spectra for $(tpy)_2$Ir(acac) and $(ppy)_2$Ir(acac) are identical. The absorption spectrum for $(bzq)_2$Ir(acac) as well as the emission spectra for $(bzq)_2$Ir(acac) and Ir$(bzq)_3$ are shown in part b. Spectra for $(bt)_2$Ir(LX), LX = acac, pic, sal, are shown in part c. Samples were in degassed 2-MeTHF solutions, measured at room temperature.

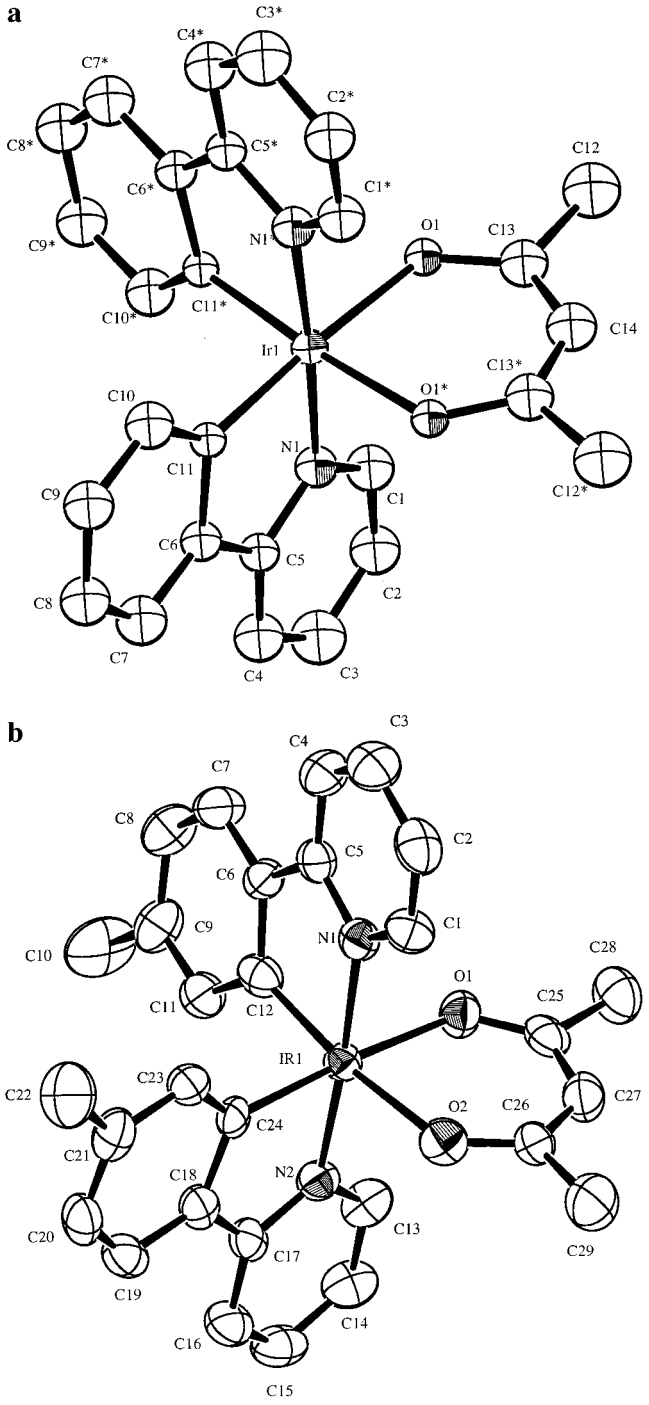

Figure 3. ORTEP drawings of (*ppy*)Ir_2(acac) (a) and (*tpy*)Ir_2(acac) (b). The thermal ellipsoids for both images represent a 50% probability limit.

plexes as well those given for other mononuclear complexes with the "ppy_2Ir" fragment.[22,23] The Ir−N bond lengths also fall within the range of values given for complexes with a "ppy_2-Ir" fragment and a *trans*-N,N′ disposition of pyridyl ligands (1.98(1)−2.07(1) Å). The Ir−N bonds are shorter than the value of 2.132 Å observed in *fac*-Ir(*tpy*)$_3$, which has all pyridyl groups trans to phenyl groups, consistent with the strong trans influence of phenyl groups. The Ir−O bond lengths of 2.146(6) and 2.161(4) Å are longer than the mean Ir−O value of 2.088 Å reported in the Cambridge Crystallographic Database[24] and

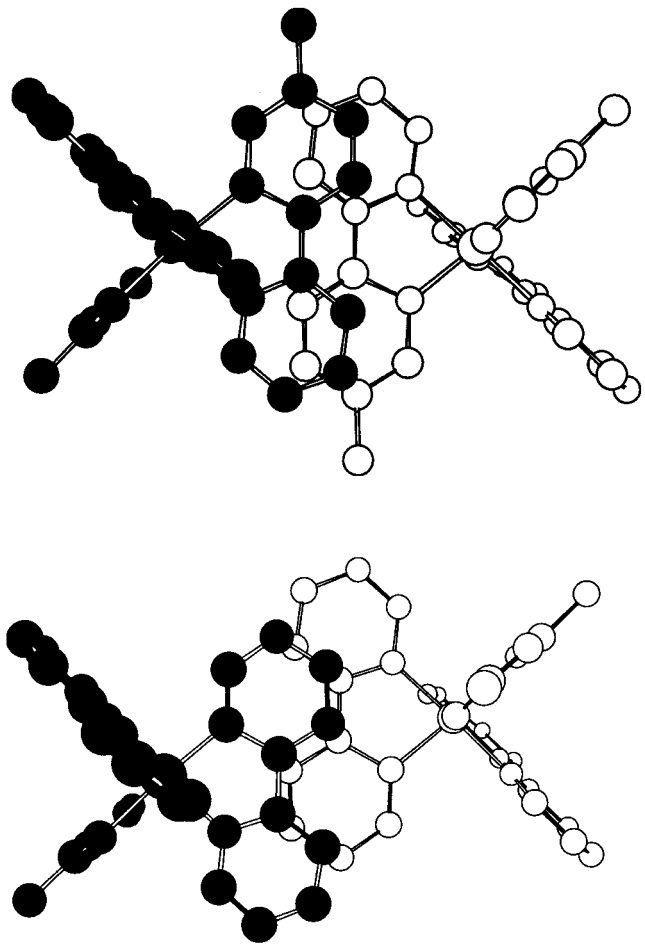

Figure 4. Crystal packing for (*tpy*)$_2$Ir(acac) (top) and (*ppy*)$_2$Ir(acac) (bottom). The molecule in the foreground is shown in black. The $\pi-\pi$ spacing between the arylpyridine (*tpy* or *ppy*) ligands of adjacent molecules is 3.4 and 3.5 Å for the *tpy* and *ppy* complexes, respectively.

reflect the large trans influence of the phenyl groups. All other bond lengths and angles within the chelate ligands are typical for cyclometalated *ppy*[17,22,23] and acac ligands bound to Ir(III).[25−27]

The crystal packing of (*tpy*)$_2$Ir(acac) shows a nearest neighbor molecule related by a *C*2 rotation that positions the pyridyl rings over the aryl rings of adjacent molecules, as shown in Figure 4 (top). The aromatic ring systems of the dyads have a significant degree of $\pi-\pi$ overlap with a ca. 3.4 Å face−face separation between the adjacent ring planes. A similar dyad formation also occurs in the crystal packing of (*ppy*)$_2$Ir(acac), albeit with a lesser degree of *ppy* ligand overlap relative to *tpy* ligands and a separation of ca. 3.5 Å between the aromatic ring systems, Figure 4 (bottom). On the basis of the higher degree of spatial overlap and closer face−face spacing of the *tpy* ligands, relative to the *ppy* ligands, we expect the $\pi-\pi$ interaction to be greater for (*tpy*)$_2$Ir(acac).

The distance separating the aromatic rings in the solid state dimers is well within range for electronic interaction between the adjacent π systems.[28] Consequently, despite having nearly

(22) Urban, R.; Krämer, R.; Mihan, S.; Polborn, K.; Wagner, B.; Beck, W. *J. Organomet. Chem.* **1996**, *517*, 191.
(23) Neve, F.; Crispini, A. *Eur. J. Inorg. Chem.* **2000**, 1039.
(24) Allen, F. H.; Davies, J. E.; Galloy, J. J.; Johnson, O.; Kennard, O.; Macrae, C. F.; Mitchell, E. M.; Mitchell, G. F.; Smith, J. M.; Watson, D. G. *J. Chem. Inf. Comput. Sci.* **1991**, *31*, 187.
(25) Esteruelas, M. A.; Lahoz, F. J.; Oñate, E.; Oro, L. A.; Rodríguez, L. *Organometallics* **1996**, *15*, 823.
(26) Papenfuhs, B.; Mahr, N.; Werner, H. *Organometallics* **1993**, *12*, 4244.
(27) Bezman, S. A.; Bird, P. H.; Fraser, A. R.; Osborn, J. A. *Inorg. Chem.* **1980**, *19*, 3755.

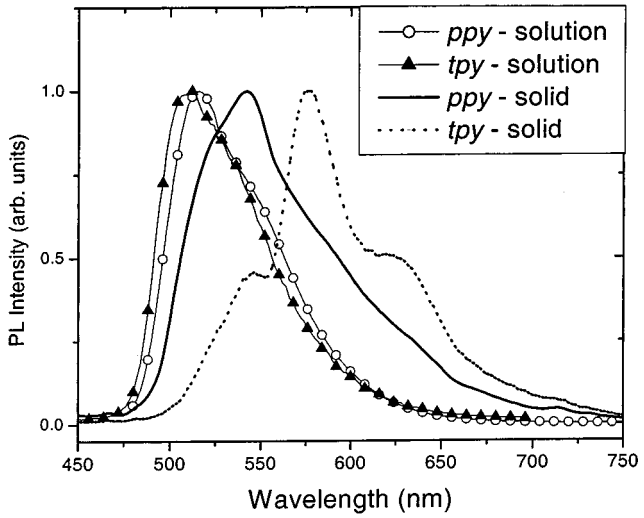

Figure 5. Solution (CH_2Cl_2) and solid state photoluminescence spectra of (*ppy*)Ir_2(acac) and (*tpy*)Ir_2(acac). The spectra were recorded at room temperature; however, cooling the samples to 77 K does not significantly alter the spectra.

identical solution absorption and emission properties, the two complexes exhibit pronounced differences in their solid state luminescence spectra (Figure 5). Powdered samples of both complexes are an indistinguishable yellow color. Powdered $(ppy)_2$Ir(acac) luminesces yellow-green with a spectrum that is broader and red-shifted ($\lambda_{max} = 540$ nm) relative to the solution spectrum, while powdered $(tpy)_2$Ir(acac) exhibits an orange emission that is more structured than that of $(ppy)_2$Ir(acac) and has a maximum at 575 nm. The shift to lower emission energy for solid $(tpy)_2$Ir(acac) versus solid $(ppy)_2$Ir(acac) correlates with the greater degree of π overlap present in the dimeric units of the former complex.[29] Face to face $\pi-\pi$ interactions between aromatic molecules in the solid state often lead to a broad and featureless luminescence that is red-shifted from the emission that occurs in dilute solution and is typically ascribed to excimer formation.[30] Excimer formation has been reported in several examples of square planar Pt(diimine) complexes;[31−33] however, the influence of π stacking on the emission properties of octahedral complexes is less well documented.[34] While the luminescence from solid $(ppy)_2$Ir(acac) is characteristic of excimer emission, the structured luminescence from $(tpy)_2$Ir(acac) suggests a different mechanism, perhaps originating from ground state dimers which act as luminescent traps.

Conclusion

Iridium tris-chelates have high phosphorescence efficiency and microsecond lifetimes, which make them ideal for OLED applications.[10] However, the synthesis of a large variety of these complexes is difficult due to steric and electronic effects of the ligands. Here it has been shown that a facile route to a variety of phosphorescent compounds exists through chloride-bridged dimers. These complexes have the general formula $\underline{C\wedge N}_2$Ir(LX), where $\underline{C\wedge N}$ is a cyclometalating ligand and LX is a monoanionic bidentate ligand. These complexes give good phosphorescence efficiencies at room temperature and have luminescent lifetimes of 1−5 μs. The absorption and emission spectra of the $\underline{C\wedge N}_2$Ir(LX) complexes are very similar to the spectra of the chloride-bridged dimers and mononuclear cationic ($\underline{C\wedge N}_2$Ir(bpy)$^+$) complexes leading to the conclusion that the emission is mainly due to the "$\underline{C\wedge N}_2$Ir" fragment. We have recently prepared organic LEDs with these complexes as emissive dopants and achieved quantum efficiencies comparable to those of devices with Ir$(ppy)_3$ dopants. This LED work will be reported elsewhere.[35]

Acknowledgment. We thank Universal Display Corporation, the Defense Advanced Research Projects Agency, and the National Science Foundation for financial support of this work.

Supporting Information Available: Crystal data, structure refinement, atomic coordinates, bond distances, bond angles, and anisotropic displacement parameters ((*tpy*)$_2$Ir(acac) only) for (*ppy*)$_2$Ir(acac) and (*tpy*)$_2$Ir(acac) and the indexed powder patterns for (*ppy*)$_2$Ir(acac) and (*tpy*)$_2$Ir(acac). This material is available free of charge via the Internet at http://pubs.acs.org.

IC0008969

(28) Hunter, C. A.; Sander, J. K. M. *J. Am. Chem. Soc.* **1990**, *112*, 5525.
(29) An alternate explanation involves the formation of aggregates in the powered sample, which are not present in solution or in the crystals examined by X-ray diffraction. The powder X-ray diffraction patterns for the *ppy* and *tpy* complexes exclude this possibility. Both complexes give well-resolved powder patterns, which can be indexed to the same unit cell found for single crystals of the same complexes. The measured powder patterns and the fits to the single-crystal unit cell parameters are given in the Supporting Information. Spectroscopic analysis of solutions of the complexes (NMR, UV−vis, and emission) match those expected for (*ppy*)$_2$Ir(acac) and (*tpy*)$_2$Ir(acac).
(30) Birks, J. B. *Photophysics of Aromatic Molecules;* Wiley-Interscience: New York, 1970.
(31) Lai, S.-W.; Chan, M. C. W.; Cheung, K.-K.; Che, C.-M. *Inorg. Chem.* **1999**, *38*, 4262.
(32) Bailey, J. A.; Hill, M. G.; Marsh, R. E.; Miskowski, V. M.; Schaefer, W. P.; Gray, H. B. *Inorg. Chem.* **1995**, *34*, 4591
(33) Miskowski, V. M.; Houlding, V. H. *Inorg. Chem.* **1989**, *28*, 1529.
(34) Alcock, N. W.; Barker, P. R.; Haider, J. M.; Hannon, M. J.; Painting, C. L.; Pikramenou, Z.; Plummer, E. A.; Rissanen, K.; Saarenketo, P. *J. Chem. Soc., Dalton Trans.* **2000**, 1447.
(35) Lamansky, S.; Djurovich, P.; Murphy, D.; Abdel-Razzaq, F.; Adachi, C.; Burrows, P. E.; Forrest, S. R.; Thompson, M. E. Submitted.